

1 EMPress enables tree-guided, interactive, and exploratory 2 analyses of multi-omic datasets

3 Kalen Cantrell^{*,1,2}, Marcus W. Fedarko^{*,1,2}, Gibraan Rahman³, Daniel McDonald⁴, Yimeng
4 Yang², Thant Zaw², Antonio Gonzalez⁴, Stefan Janssen⁵, Mehrbod Estaki⁴, Niina Haiminen⁶,
5 Kristen L. Beck⁷, Qiyun Zhu^{4,8}, Erfan Sayyari^{2,9}, Jamie Morton¹⁰, Anupriya Tripathi⁴, Julia M.
6 Gauglitz¹⁵, Clarisse Marotz^{4,11}, Nathaniel L. Matteson¹³, Cameron Martino^{2,3,4}, Jon G.
7 Sanders¹⁶, Anna Paola Carrieri¹⁴, Se Jin Song², Austin D. Swafford², Pieter C. Dorrestein^{2,15},
8 Kristian G. Andersen¹³, Laxmi Parida⁶, Ho-Cheol Kim⁷, Yoshiki Vázquez-Baeza², Rob
9 Knight^{1,2,4,12}.

10

11 *Contributed Equally.

12 ¹Department of Computer Science, Jacobs School of Engineering, University of California, San
13 Diego.

14 ²Center for Microbiome Innovation, Jacobs School of Engineering, University of California, San
15 Diego.

16 ³Bioinformatics and Systems Biology Program, University of California, San Diego.

17 ⁴Department of Pediatrics, School of Medicine, University of California, San Diego.

18 ⁵Algorithmic Bioinformatics, Justus Liebig University Giessen, Germany.

19 ⁶IBM T. J. Watson Research Center, Yorktown Heights, New York.

20 ⁷IBM Almaden Research Center, San Jose, California.

21 ⁸Present Address: Biodesign Center for Fundamental and Applied Microbiomics, Arizona State
22 University, Arizona.

23 ⁹Department of Electrical and Computer Engineering, University of California, San Diego.

24 ¹⁰Center for Computational Biology, Flatiron Institute, Simons Foundation, New York, NY, USA.

25 ¹¹Scripps Institution of Oceanography, University of California, San Diego.

26 ¹²Department of Bioengineering, University of California, San Diego.

27 ¹³Scripps Research Institute, San Diego, California.

28 ¹⁴IBM Research, The Hartree Centre, Daresbury, UK

29 ¹⁵Collaborative Mass Spectrometry Innovation Center, Skaggs School of Pharmacy and
30 Pharmaceutical Sciences, University of California, San Diego.

31 ¹⁶Cornell Institute for Host-Microbe Interaction and Disease, Cornell University, Ithaca

32 Abstract

33 Standard workflows for analyzing microbiomes often include the creation and curation of
34 phylogenetic trees. Here we present EMPress, an interactive tool for visualizing trees in the
35 context of microbiome, metabolome, etc. community data scalable beyond modern large
36 datasets like the Earth Microbiome Project. EMPress provides novel functionality—including
37 ordination integration and animations—alongside many standard tree visualization features, and
38 thus simplifies exploratory analyses of many forms of ‘omic data.

39

40

41 Main Text

42

43 The increased availability of sequencing technologies and automation of molecular methods
44 have enabled studies of unprecedented scale [1] prompting the creation of tools better suited to
45 store, analyze [2], and visualize [3] studies of this magnitude. Many of these tools, such as [4, 5,
46 6, 7], use phylogenies detailing the evolutionary relationships among features or dendograms
47 that organize features in a hierarchical structure (e.g. clustering of mass spectra) [8]. The
48 challenge of enabling fully interactive analyses stems from the disconnect between feature-level
49 tools and dataset-level tools; few can interactively integrate multiple representations of the data
50 [9], and to our knowledge none scale to display large datasets. This is a key unresolved
51 challenge for the field: to allow researchers to contextualize community-level patterns
52 (groupings of samples) together with feature-level structure, i.e. which features lead to the
53 groupings explained in a given sample set.

54

55 Here, we introduce EMPress (<https://github.com/biocore/empress>), an open-source (BSD 3-
56 clause), interactive and scalable phylogenetic tree viewer accessible as a QIIME 2 [2] plugin.
57 EMPress is built around the high-performance balanced parentheses tree data structure [10],
58 and uses a hardware-accelerated WebGL-based rendering engine that allows EMPress to
59 visualize trees with hundreds of thousands of nodes using a laptop's web browser (Methods).
60 By integrating EMPress with the widely-used EMPeror software [3] within QIIME 2, EMPress
61 can simultaneously visualize a phylogenetic tree of features in a study coupled with an
62 ordination of the same study's samples. User actions in one visualization, such as selecting a
63 set of samples in the ordination, update the other, providing context that would not be easily
64 accessible with independent visualizations. This tight integration between displays streamlines
65 several use-cases elaborated below that previously required manual investigation or writing
66 custom scripts.

67

68 EMPress visualizations can be created solely from a tree, or users can provide additional
69 metadata files and a feature table to augment the tree. Using these common data files, users
70 can interactively configure many visual attributes in the tree (see Methods and Figures for
71 examples).

72

73 Rather than providing a programmatic interface for the procedural generation of styled
74 phylogenetic trees [11, 12, FigTree (<http://tree.bio.ed.ac.uk/software/figtree/>)], EMPress
75 provides an interactive environment to support exploratory feature- and sample-level tree-based
76 analyses. Many use-cases supported in EMPress accommodate community analysis tasks; this
77 differs from Anvi'o [13] which is centered on the analysis of metagenomic assembled-genomes,
78 pangenomes, etc.. PHYLOViZ [9], SigTree [14], and iTOL [15] are similar to EMPress in terms
79 of their implementation (PHYLOViZ Online also uses WebGL), and/or use-cases (SigTree is
80 mostly used to visualize differential abundance patterns, and iTOL supports the visualization of
81 QIIME 2 tree artifacts). EMPress stands out in its scalability: iTOL claims trees with more than

82 10,000 tips to be “very large” (<https://itol.embl.de/help.cgi>), while EMPress readily supports trees
83 with over hundreds of thousands of tips, as shown in Fig. 1. Many visualization customization
84 options available in EMPeror, iTOL [15] and Anvi’o [13] are immediately accessible in EMPress’
85 interface. Continuous feature metadata can be visualized in tip-level barplots as a color gradient
86 and/or by adjusting the lengths of individual tips’ barplots; categorical sample metadata
87 information can be visualized using a stacked barplot showing—for each tip—the proportion of
88 samples containing that tip stratified by category. These options are available on the user
89 interface and do not require programming or configuration files.

90
91 Ordination plots computed from UniFrac distances are often used to visualize sample clustering
92 patterns in microbiome studies. However, interpreting the patterns in these plots—and
93 determining which features influence sample group separation—is not always straightforward.
94 While biplots show information about influential features alongside samples, the phylogenetic
95 relationships of these features are not immediately obvious. EMPress aids interpretation of
96 these plots by optionally providing a unified interface where the tree and ordination
97 visualizations are displayed side-by-side and “linked” through sample and feature identifiers
98 [16]. This combination allows for novel exploratory data analysis tasks. For example, selecting a
99 group of samples in the ordination highlights nodes in the tree present in those samples, and
100 vice versa (see Methods). This integration extends to biplots: clicking feature arrows in the
101 ordination highlights their placement in the tree. Lastly, EMPress allows visualizing longitudinal
102 studies by simultaneously showing the tree nodes unique to groups of samples at each
103 individual time point during an EMPeror animation (see Methods).

104
105 Using the first data release of the Earth Microbiome Project (EMP), we demonstrate EMPress’
106 scalability by rendering a 26,035 sample ordination and a 756,377 node tree (Figure 1A). To
107 visualize the relative proportions of taxonomic groups at the phylum level, we use EMPress’
108 feature metadata coloring to highlight the top 5 most prevalent phyla (see Methods). Next, we
109 add a barplot layer showing, for each tip in the tree, the proportions of samples containing each
110 tip summarized by level 2 of the EMP ontology (Animal, Plant, Non-Saline, and Saline). Paired
111 visualizations allow us to click on a tip in the tree and view the samples that contain that feature
112 in the ordination. This functionality is useful when analyzing datasets with outliers or mislabeled
113 metadata. Tip-aligned barplots summarize environmental metadata: for example, Figure 1B
114 shows the subset of samples (4,002) with recorded pH information and a barplot layer with the
115 mean pH where each feature was found. The barplot reveals a relatively dark section near
116 many Firmicutes-classified features on the tree; in concert with histograms showing mean pH
117 for each phylum (Figure 1C), we can confirm that Firmicutes-classified features are more
118 commonly found in higher pH environments.

119
120 EMPress can be applied to various ‘omic datasets. To illustrate this versatility we reanalyzed a
121 COVID-19 metatranscriptome sequencing dataset [17], a liquid chromatography mass-
122 spectrometry (LC-MS) untargeted metabolomic food-associated dataset [8], and a 16S rRNA
123 sequencing oral microbiome dataset [18]. Despite the vastly different natures of these datasets,
124 EMPress provides meaningful functionality for their analysis and visualization. Supplemental
125 Video 1 ([supplementary-video-1.mp4](#)) shows a longitudinal exploratory analysis using EMPress

126 and EMPeror representing a subset of SARS-CoV-2 genome data from GISAID. This paired
127 visualization emphasizes the relationships in time and space among “community samples” and
128 the convergence of locales in the United States with the outbreak in Italy (See Methods). The
129 interactive nature of EMPress allows rapid visualization of strains observed in a collection of
130 samples from different geographical locations.

131
132 Figure 2A showcases Empress’ ability to identify feature clusters that are differentially abundant
133 in COVID-19 patients compared to community-acquired pneumonia patients and healthy
134 controls [17]. Clades showing KEGG enzyme code (EC) [19] annotations are collapsed at level
135 two except for lyases, highlighting feature 4.1.1.20 (carboxy-lyase diaminopimelate
136 decarboxylase) that was more abundant in COVID-19 here and in an independent
137 metaproteomic analysis of COVID-19 respiratory microbiomes [20].

138
139 Recent developments in cheminformatics enabled the analysis and visualization of small
140 molecules in the context of a cladogram [8]. Using a tree that links molecules by their structural
141 relatedness, we analyzed untargeted LC-MS/MS data from 70 food samples (see Methods).
142 With EMPress’ sample metadata barplots, we can inspect the relationship between chemical
143 annotations and food types. Figure 2B shows a tree where each tip is colored by its chemical
144 super class, and where barplots show the proportion of samples in the study containing each
145 compound by food type. This representation reveals a clade of lipids and lipid-like molecules
146 that are well represented in animal food types and seafoods. In contrast, salads and fruits are
147 broadly spread throughout the cladogram.

148
149 Lastly, in Figure 2C, we compare three differential abundance methods in an oral microbiome
150 dataset [18] as separate barplot layers on a tree. This dataset includes samples (n=32) taken
151 before and after subjects brushed their teeth (see Methods). As observed across the three
152 differential abundance tools’ outputs, all methods agree broadly on which features are
153 particularly “differential” (for example, the cluster of Firmicutes-classified sequences in the
154 bottom-right of the tree; see Methods), although there are discrepancies due to different
155 methods’ assumptions and biases.

156 Conclusions

157 By providing an intuitive interface supporting both categorically new and established
158 functionality, EMPress complements and extends the available range of tree visualization
159 software. EMPress can perform community analyses across distinct “omics” types, as
160 demonstrated here. Moving forward, facilitating the integration of multiple orthogonal views of a
161 dataset at a more generalized framework level (for example, using QIIME2’s [2] visualization
162 API) will be important as datasets continue to grow in complexity, size, and heterogeneity.

163 Acknowledgements

164 We thank members of the Knight Lab and IBM AIHL Bioinformatics team for feedback during
165 code reviews and presentations. We gratefully acknowledge the following Authors from the
166 originating laboratories responsible for obtaining the specimens and the submitting laboratories

167 where genetic sequence data were generated and shared via the GISAID Initiative, on which a
168 portion of this research is based (Supplemental Table 1).
169

170 **Funding**

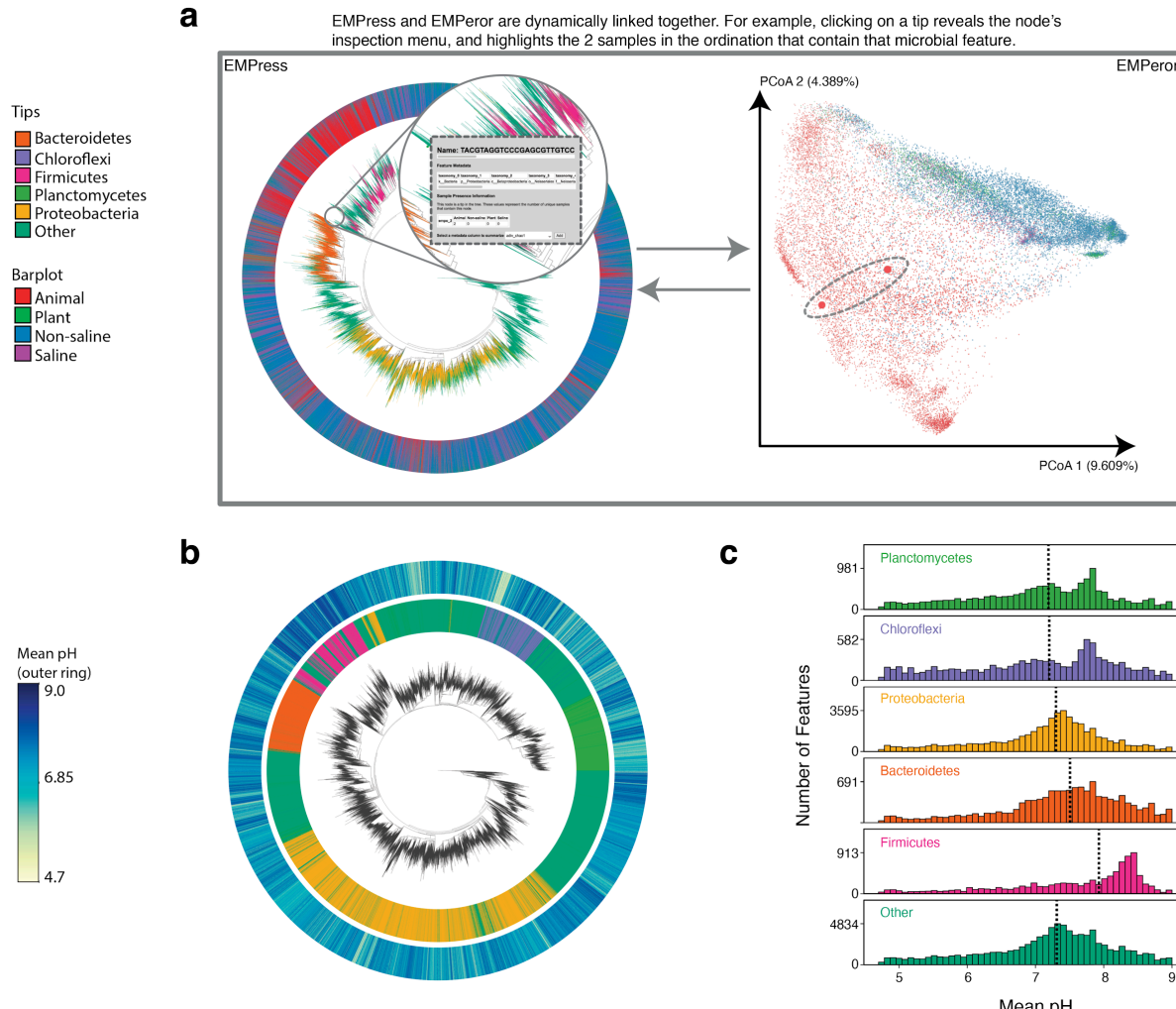
171 This work is partly supported by IBM Research AI through the AI Horizons Network and the UC
172 San Diego Center for Microbiome Innovation (to KC, MWF, JM, QZ, TZ, JS, ADS, SS, YVB,
173 RKF); CCF foundation #675191 (RK and PCD), U19 AG063744 01 (RK, JMG, PCD), CDC
174 contract #75D30120C09795 (KGA and RK), U19 AI135995 (KGA).

175 **Author Contributions**

176 KC, QZ, YY, JM, TZ, JS, and RK conceived the original idea for the project. KC, MWF, GR, DM,
177 AG, SJ, ME, YY, ES, JM, TZ, QZ, YVB wrote source code and/or documentation for the project.
178 KC, MWF, AG, YVB wrote code to facilitate integration with EMPeror. LP, HCK, SS, ADS, YVB,
179 RK managed the project. KC, MWF, GR, NH, KLB, AT, JMG, LM, APC, NLM, CM, PCD, KGA,
180 LP, YVB analyzed and interpreted the datasets presented in this paper. KC, MWF, GR, DM,
181 NH, KLB, YVB contributed text to the methods section. All the authors contributed to the final
182 version of the manuscript.

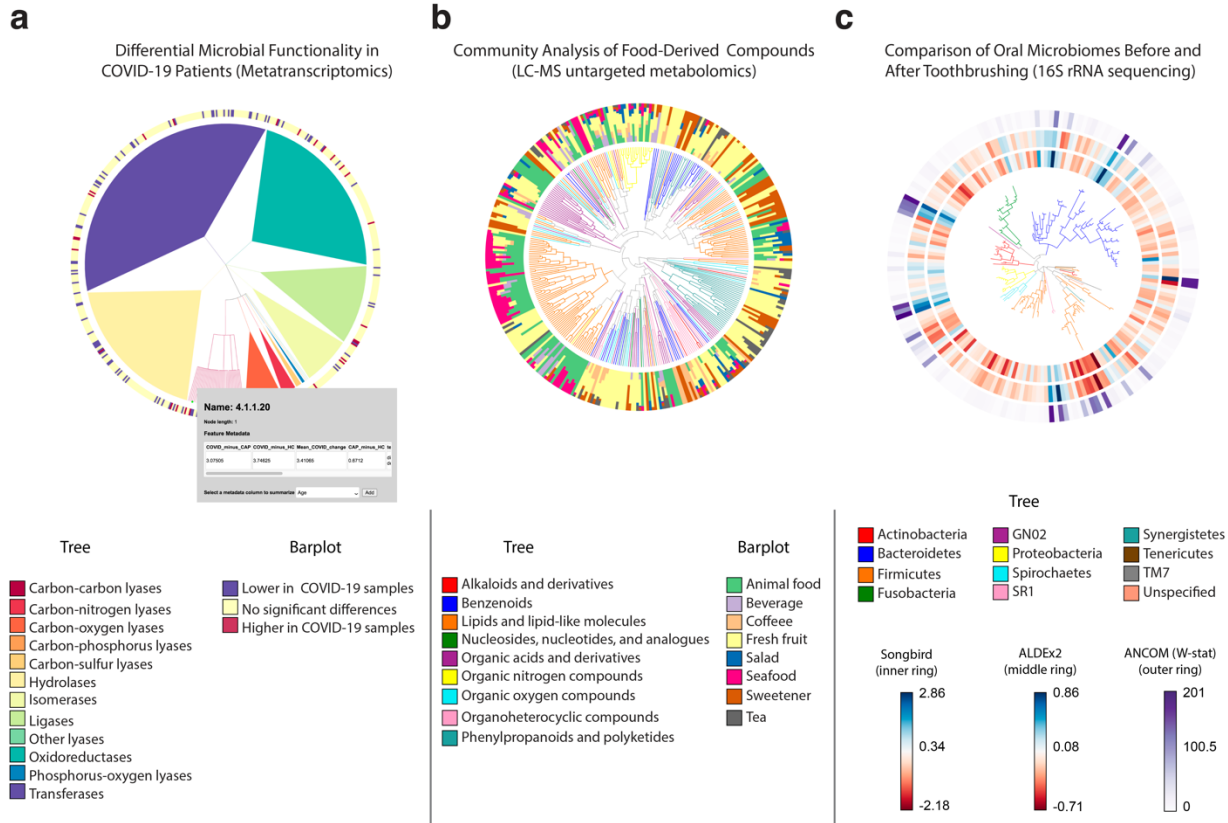
183 **Competing Interests**

184 We declare none.



185
186
187
188
189
190
191
192
193
194
195
196
197

Figure 1. Earth Microbiome Project paired phylogenetic tree (including 756,377 nodes) and unweighted UniFrac ordination (including 26,035 samples) . (a) Graphical depiction of Empress' unified interface with fragment insertion tree (left), and unweighted UniFrac sample ordination (right). Tips are colored by their phylum-level taxonomic assignment; the barplot layer is a stacked barplot describing the proportions of samples containing each tip summarized by level 2 of the EMP ontology. Inset shows summarized sample information for a selected feature. The ordination highlights the two samples containing the tip selected in the tree enlarged to show their location. **(b)** Subset of EMP samples with pH information: the inner barplot ring shows the phylum-level taxonomic assignment, and the outer barplot ring represents the mean pH of all the samples where each tip was observed **(c)** pH distributions summarized by phylum-level assignment with median pH indicated by dotted lines. Interactive figures can be accessed [here](#).



198
199
200
201
202
203
204
205
206
207
208
209
210
211
212
213
214
215
216
217

Figure 2. EMPress is a versatile exploratory analysis tool adaptable to various -omics data types.

(a) RoDEO differential abundance scores of microbial functions from metatranscriptomic sequencing of COVID-19 patients (n=8), community-acquired pneumonia patients (n=25), and healthy control subjects (n=20). The tree represents the four-level hierarchy of the KEGG enzyme code. The barplot colors significantly differentially abundant features (p<0.05) in COVID-19 patients. Clicking on a tip produces a pop-up insert tabulating the name of the feature, its hierarchical ranks, and any feature annotations.

(b) Global FoodOmics Project LC-MS data. Stacked barplots indicate the proportions of samples (n=70) (stratified by food) containing the tips in an LC-MS Qemistree of food-associated compounds, with tip nodes colored by their chemical superclass.

(c) *de novo* tree constructed from 16S rRNA sequencing data from 32 oral microbiome samples. Samples were taken before (n=16) and after (n=16) subjects (n=10) brushed their teeth; each barplot layer represents a different differential abundance method's measure of change between before- and after-brushing samples. The innermost layer shows estimated log-fold changes produced by Songbird; the middle layer shows effect sizes produced by ALDE2; and the outermost layer shows the W-statistic values produced by ANCOM (see Methods). The tree is colored by tip nodes' phylum-level taxonomic classifications. Interactive figures can be accessed [here](#).

218 References

219 1. Thompson, L. R. *et al.* A communal catalogue reveals Earth's multiscale microbial
220 diversity. *Nature* **551**, 457–463 (2017).

221 2. Bolyen, E. *et al.* Reproducible, interactive, scalable and extensible microbiome data
222 science using QIIME 2. *Nat. Biotechnol.* **37**, 852–857 (2019).

223 3. Vázquez-Baeza, Y., Pirrung, M., Gonzalez, A. & Knight, R. EMPeror: a tool for
224 visualizing high-throughput microbial community data. *Gigascience* **2**, 16 (2013).

225 4. Lozupone, C. & Knight, R. UniFrac: a new phylogenetic method for comparing microbial
226 communities. *Appl. Environ. Microbiol.* **71**, 8228–8235 (2005).

227 5. Washburne, A. D. *et al.* Phylogenetic factorization of compositional data yields lineage-
228 level associations in microbiome datasets. *PeerJ* **5**, e2969 (2017).

229 6. Silverman, J. D., Washburne, A. D., Mukherjee, S. & David, L. A. A phylogenetic
230 transform enhances analysis of compositional microbiota data. *Elife* **6**, (2017).

231 7. Morton, J. T. *et al.* Balance Trees Reveal Microbial Niche Differentiation. *mSystems* **2**,
232 (2017).

233 8. Tripathi, A. *et al.* Chemically-informed Analyses of Metabolomics Mass Spectrometry
234 Data with Qemistree. *bioRxiv* 2020.05.04.077636 (2020)
235 doi:[10.1101/2020.05.04.077636](https://doi.org/10.1101/2020.05.04.077636).

236 9. Nascimento, M. *et al.* PHYLOViZ 2.0: providing scalable data integration and
237 visualization for multiple phylogenetic inference methods. *Bioinformatics* **33**, 128–129
238 (2017).

239 10. Cordova, J. & Navarro, G. Simple and efficient fully-functional succinct trees. *Theoretical
240 Computer Science* **656**, 135–145 (2016).

241 11. Yu, G. Using ggtree to Visualize Data on Tree-Like Structures. *Curr Protoc
242 Bioinformatics* **69**, e96 (2020).

243 12. Huerta-Cepas, J., Serra, F. & Bork, P. ETE 3: Reconstruction, Analysis, and
244 Visualization of Phylogenomic Data. *Mol. Biol. Evol.* **33**, 1635–1638 (2016).

245 13. Eren, A. M. *et al.* Anvi'o: an advanced analysis and visualization platform for 'omics data.
246 *PeerJ* **3**, e1319 (2015).

247 14. Stevens, J. R., Jones, T. R., Lefevre, M., Ganesan, B. & Weimer, B. C. SigTree: A
248 Microbial Community Analysis Tool to Identify and Visualize Significantly Responsive
249 Branches in a Phylogenetic Tree. *Comput Struct Biotechnol J* **15**, 372–378 (2017).

250 15. Letunic, I. & Bork, P. Interactive Tree Of Life (iTOL) v4: recent updates and new
251 developments. *Nucleic Acids Res* **47**, W256–W259 (2019).

252 16. Becker, R. A., Cleveland, W. S. & Wilks, A. R. Dynamic Graphics for Data Analysis.
253 *Statist. Sci.* **2**, 355–383 (1987).

254 17. Shen, Z. *et al.* Genomic Diversity of Severe Acute Respiratory Syndrome–Coronavirus 2
255 in Patients With Coronavirus Disease 2019. *Clin Infect Dis* **71**, 713–720 (2020).

256 18. Morton, J. T. *et al.* Establishing microbial composition measurement standards with
257 reference frames. *Nat Commun* **10**, 2719 (2019).

258 19. Kanehisa, M. Enzyme Annotation and Metabolic Reconstruction Using KEGG. *Methods
259 Mol. Biol.* **1611**, 135–145 (2017).

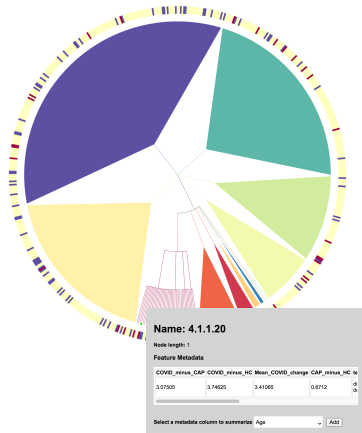
260 20. Maras, J. S. *et al.* Multi-Omics integration analysis of respiratory specimen characterizes
261 baseline molecular determinants associated with COVID-19 diagnosis. *medRxiv*
262 2020.07.06.20147082 (2020) doi:[10.1101/2020.07.06.20147082](https://doi.org/10.1101/2020.07.06.20147082).

263

264

a

Differential Microbial Functionality in COVID-19 Patients (Metatranscriptomics)



Tree

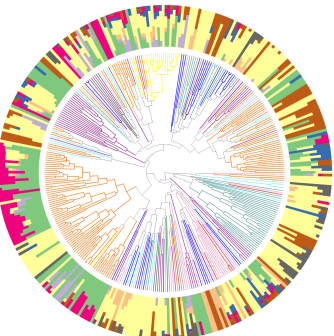
- Carbon-carbon lyases
- Carbon-nitrogen lyases
- Carbon-oxygen lyases
- Carbon-phosphorus lyases
- Carbon-sulfur lyases
- Hydrolases
- Isomerases
- Ligases
- Other lyases
- Oxidoreductases
- Phosphorus-oxygen lyases
- Transferases

Barplot

- Lower in COVID-19 samples
- No significant differences
- Higher in COVID-19 samples

b

Community Analysis of Food-Derived Compounds (LC-MS untargeted metabolomics)



Tree

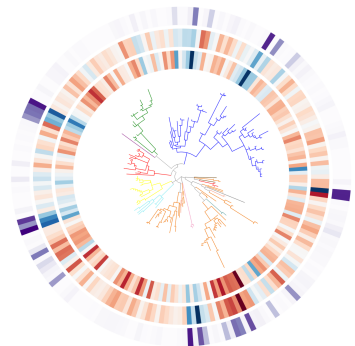
- Alkaloids and derivatives
- Benzenoids
- Lipids and lipid-like molecules
- Nucleosides, nucleotides, and analogues
- Organic acids and derivatives
- Organic nitrogen compounds
- Organic oxygen compounds
- Organoheterocyclic compounds
- Phenylpropanoids and polyketides

Barplot

- Animal food
- Beverage
- Coffeee
- Fresh fruit
- Salad
- Seafood
- Sweetener
- Tea

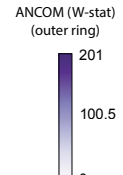
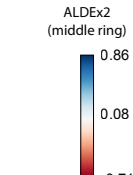
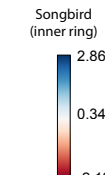
c

Comparison of Oral Microbiomes Before and After Toothbrushing (16S rRNA sequencing)



Tree

Actinobacteria	GN02	Synergistetes
Bacteroidetes	Proteobacteria	Tenericutes
Firmicutes	Spirochaetes	TM7
Fusobacteria	SR1	Unspecified



a

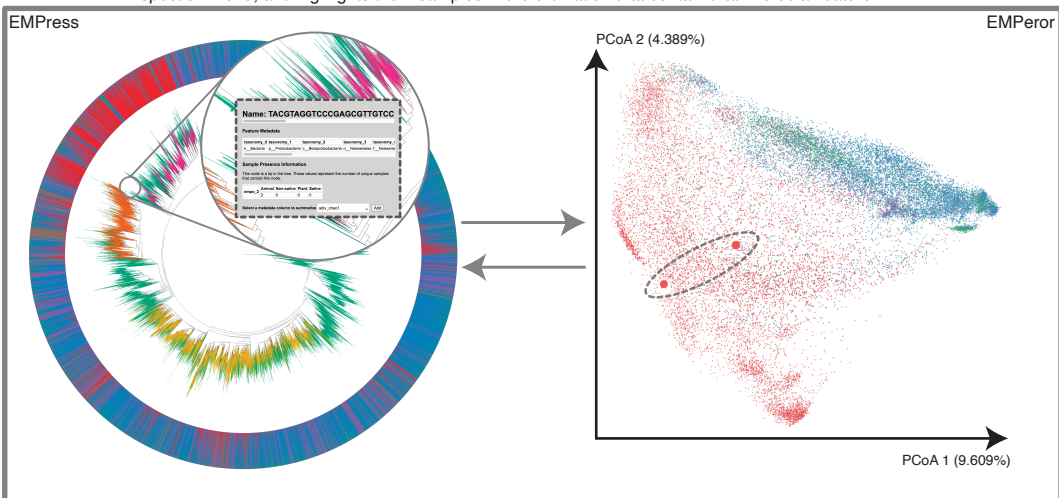
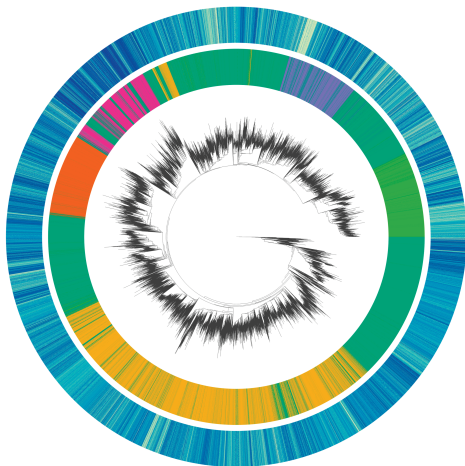
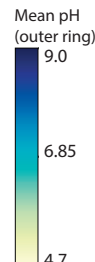
EMPress and EMPeror are dynamically linked together. For example, clicking on a tip reveals the node's inspection menu, and highlights the 2 samples in the ordination that contain that microbial feature.

Tips

- Bacteroidetes
- Chloroflexi
- Firmicutes
- Planctomycetes
- Proteobacteria
- Other

Barplot

- Animal
- Plant
- Non-saline
- Saline

**b****c**